

# Unlocking the Latent Antimicrobial Potential of Biomimetically Synthesized Inorganic Materials

Matthew B. Dickerson, Wanda J. Lyon, William E. Gruner, Peter A. Mirau, Michael L. Jespersen, Yunnan Fang, Kenneth H. Sandhage, and Rajesh R. Naik\*

Inspired by biomineralization, biomimetic approaches utilize biomolecules and synthetic analogs to produce materials of controlled chemistry, morphology, and function under relatively benign conditions. A common characteristic of biological and biomimetic mineral-forming processes is the generation of mineral/biomolecule nanocomposites. In this work, it is demonstrated that a facile chemical reaction may be utilized to halogenate the nitrogen-containing moieties of the organics entrapped within bio-inorganic composites to yield halamine compounds. This process provides rapid and potent bactericidal activity to biomimetically and biologically produced materials that otherwise lack such functionality. Additionally, bio-inorganic composites containing the chlorinated peptide protamine are effective in rapidly neutralizing *Bacillus* spores ( $\geq 99.97\%$  reduction in colony forming units within 10 min). The straightforward nature of the described process, and the efficacy of halamine compounds in neutralizing biological and chemical agents, provide new applicability to biogenic and biomimetic materials.

extracted from these organisms have been utilized to induce the formation of silica under relatively benign conditions in vitro.<sup>[7,8]</sup> Proteins associated with sponge and diatom biosilicification have also been used to synthesize inorganic materials (e.g.,  $\text{TiO}_2$ ) not typically produced by these organisms.<sup>[9,10]</sup> Synthetic biomolecules have also been found capable of mediating the syntheses of a multitude of inorganics in vitro.<sup>[1,2]</sup> Similar to the biological materials systems they are intended to mimic (e.g., silicatein/silica spicules)<sup>[5,6]</sup>, the products of bio-inspired materials synthesis studies are typically not monolithic inorganic structures. Rather, these biomimetically produced materials are composites consisting of an inorganic phase and the mediating biomolecules.<sup>[1]</sup>

The hybrid nature of materials produced through bio-inspired mineraliza-

## 1. Introduction

Biomimetic materials synthesis techniques seek to explore the methodologies by which biology controllably produces functional inorganic materials and structures through processes collectively known as biomineralization.<sup>[1,2]</sup> Biomineralizing organisms, such as diatoms and sponges, utilize specialized biomolecules to reproducibly create well-defined silica structures under cellular conditions.<sup>[3–6]</sup> Indeed, biomolecules

tion processes presents opportunities to generate materials that retain the functionality of the entrapped biomolecule.<sup>[11]</sup> For example, ceramic composites with bactericidal activity have been produced when the synthesis-mediating and subsequently entrapped biomolecules were antimicrobial enzymes or peptides.<sup>[12,13]</sup> The bactericidal activity of such materials has also been augmented through the biomolecule-directed growth of antimicrobial inorganics (e.g., silver nanoparticles).<sup>[14–16]</sup> Though such approaches have been successfully used to produce bactericidal materials, the design of biomimetically synthesized antimicrobial materials is currently constrained to incorporating molecules or inorganic materials (e.g., lysozyme or silver) possessing explicit antimicrobial activity. Additionally, while lysozyme-, antimicrobial peptide-, and silver-based composites have been efficacious in killing vegetative bacteria, these systems are ineffective against bacterial spores.<sup>[17]</sup>

The development of materials that can neutralize bacterial spores is of importance, as infections from some pathogenic bacteria, including *Bacillus anthracis* and *Clostridium difficile*, may initiate through contact with spores.<sup>[18,19]</sup> Bacterial spores are specialized types of dormant cells that can preserve bacteria for long periods of time in the ambient environment and are resistant to common chemical disinfectants.<sup>[17,18]</sup> Among the limited number of compounds that exhibit sporocidal activity at room temperature are the halamines. Halamines are compounds that contain one or more nitrogen-halogen (e.g.,

Dr. M. B. Dickerson, Dr. P. A. Mirau, Dr. M. L. Jespersen, Dr. R. R. Naik

Materials and Manufacturing Directorate  
and Human Effectiveness Directorate  
Air Force Research Laboratory  
Wright-Patterson Air Force Base, OH 45433, USA  
E-mail: Rajesh.Naik@wpafb.af.mil

Dr. W. J. Lyon, W. E. Gruner  
Human Effectiveness Directorate  
Air Force Research Laboratory  
Wright-Patterson Air Force Base, OH 45433, USA  
Dr. Y. Fang, Prof. K. H. Sandhage  
School of Materials Science and Engineering  
Georgia Institute of Technology  
Atlanta, GA 30332, USA



DOI: 10.1002/adfm.201202851



**Scheme 1.** Generalized halamine chemistry. The synthesis of a halamine compound through the chlorination of a nitrogen moiety with hypochlorous acid (forward reaction) and the regeneration of these reactants via the hydrolysis of the halamine (reverse reaction).

chlorine) covalent bonds and liberate oxidizing halogens in water (**Scheme 1**).<sup>[20]</sup> A number of nitrogen-containing specialty materials (e.g., fabrics and polymers) that can be halogenated to yield halamines have been developed over the last decade.<sup>[21–25]</sup> Though such halamine-functionalized materials can rapidly (e.g., ≤10 min) kill vegetative bacterial cells, these materials typically require hours to fully deactivate *Bacillus* spores.<sup>[21,22]</sup> In a recent study, we demonstrated that halamine-containing materials capable of killing *Bacillus* spores within minutes of contact can be produced through the chlorination of silk, a protein-based and nitrogen-rich material.<sup>[26]</sup>

Here, we demonstrate that the nitrogen-containing moieties of the biomolecules or polymers entrapped within biomimetically or biologically synthesized inorganics provide unexploited reaction sites that can be utilized to add rapid and potent antimicrobial activity to a vast array of materials systems. Irrespective of sequence, the polypeptide constituents of biomimetically produced materials have an amide-based backbone that may be chlorinated to yield halamines. In addition to the peptide bond, the entrapped peptide/protein may also possess sites for halamine formation in the side chains of specific amino acid residues. The use of this facile chemistry to add halamine functionality to the macromolecular species entrapped within biologically and biomimetically synthesized inorganics provides a straightforward means of imparting bactericidal and sporicidal functionality to materials that would otherwise lack such activity.

## 2. Results and Discussion

### 2.1. Synthesis, Chlorination, and Characterization of Peptide/Inorganic Composite Materials

The addition of antimicrobial activity to biomimetically synthesized materials via the chlorination of nitrogen-containing moieties was first explored with protamine/silica (pSiO<sub>2</sub>) composites. Protamine was selected as an early candidate for study, because this peptide is highly enriched in nitrogen-containing arginine residues and has recently been utilized in the bioenabled production of silica and titania.<sup>[27,28]</sup> pSiO<sub>2</sub> precipitates were produced through the protamine-mediated condensation of silicic acid in 100 mM phosphate-citrate buffered solution (pH 7). The pSiO<sub>2</sub> materials produced under these reaction conditions are spherical particles with diameters of ≈700 nm (**Figure 1a** and Supporting Information Figure S1). Purified pSiO<sub>2</sub> powders were chlorinated in a 10% (v/v) Clorox bleach (NaOCl) solution that contained NaCl and was slightly acidified (pH 5) with acetic acid.<sup>[26]</sup> Following reaction in this chlorinating solution, the morphology of the pSiO<sub>2</sub> powders was unchanged from that of the original materials, remaining as ≈700 nm diameter spherical particles (**Figure 1b** and

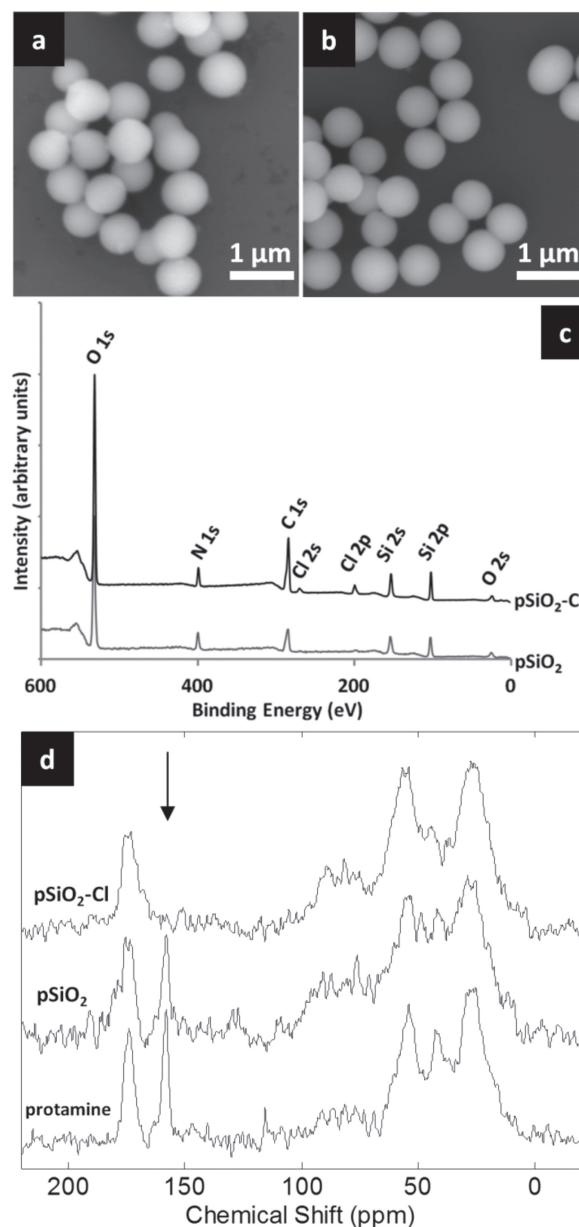


**Figure 1.** Characterization of protamine/SiO<sub>2</sub> materials before and after chlorination. SEM of a) pSiO<sub>2</sub> and b) pSiO<sub>2</sub>-Cl. c) Chemical analyses by XPS of pSiO<sub>2</sub> (bottom spectrum, gray line) and pSiO<sub>2</sub>-Cl (top spectrum, black line). Intensity values of the pSiO<sub>2</sub>-Cl XPS spectrum are offset for clarity. d) ssNMR of protamine, pSiO<sub>2</sub>, and pSiO<sub>2</sub>-Cl. The arrow in (d) highlights the peak position associated with the guanidinium carbon of the arginine side chain.

Supporting Information Figure S2). Chemical analyses of the chlorinated protamine/silica composites (pSiO<sub>2</sub>-Cl) by X-ray photoelectron spectroscopy (XPS) and energy-dispersive X-ray spectroscopy (EDS) characterization indicated that these materials had compositions similar to those of the initial pSiO<sub>2</sub> materials (containing Si, O, C, and N) plus the additional element Cl (**Figure 1c** and Supporting Information Figure S1,S2). Changes occurring to pSiO<sub>2</sub> materials as a result of chlorination are also evident when comparing the solid state NMR (ssNMR)

spectra of protamine, pSiO<sub>2</sub>, and pSiO<sub>2</sub>-Cl. As presented in Figure 1d, the ssNMR spectra of protamine and pSiO<sub>2</sub> display a prominent peak ( $\approx 160$  ppm) corresponding to the guanidinium carbon of the arginine side chain. This peak is absent in the spectrum of pSiO<sub>2</sub>-Cl, indicating that a major change, such as halamine formation, has occurred in the chemical environment of this carbon atom. This change in the spectrum of pSiO<sub>2</sub>-Cl is not caused by the loss of protamine from the sample, as peaks corresponding to the C $\alpha$ - and side chain aliphatic carbons of arginine ( $\approx 56$ – $27$  ppm) that are evident in protamine and pSiO<sub>2</sub> spectra are retained in the pSiO<sub>2</sub>-Cl spectrum. The chlorination of the arginine side chain and the associated loss of positive surface charges were also observed through differences in the zeta potentials of these materials before and after chlorination ( $36.8 \pm 11.2$  mV and  $-24 \pm 6.9$  mV for pSiO<sub>2</sub> and pSiO<sub>2</sub>-Cl, respectively). The active Cl content of the pSiO<sub>2</sub>-Cl materials was assessed by iodometric titration and found to be dependent on chlorination time for up to 15 min, after which saturation was observed (Supporting Information Figure S3). The pSiO<sub>2</sub> powder chlorinated for 1 h (the longest reaction time tested) contained  $6.50 \pm 0.28$  mmol Cl/g material. Consistent with this result, the Cl content of 1 h reacted pSiO<sub>2</sub>-Cl was determined to be  $23.9 \pm 0.3$  wt% Cl (i.e.,  $6.7 \pm 0.1$  mmol Cl/g material) by combustion/elemental analysis. Further chemical characterization of the synthesized pSiO<sub>2</sub> particles by CHN elemental analysis indicated that these powders were composed of 11.2 wt% N (i.e.,  $8.0 \pm 0.5$  mmol N/g material) and thus possess a Cl to N ratio of 0.8:1. Control experiments conducted with pSiO<sub>2</sub> materials in which the protamine component had been removed by pyrolysis prior to chlorination were not found to contain Cl by EDS, XPS, or iodometric titration (Supporting Information Figure S4). Taken together, the results of chemical analyses by EDS, XPS, and ssNMR, along with the lack of Cl in the control sample, clearly indicated that protamine is essential for the charging of pSiO<sub>2</sub> with Cl.

The quantity of Cl loaded into pSiO<sub>2</sub> represents a significant increase over that previously achieved for silk fabrics chlorinated for 1 h ( $1.76 \pm 0.03$  mmol Cl/g).<sup>[26]</sup> The considerable Cl carrying capacity of pSiO<sub>2</sub> arises from the relatively large proportion of protamine (35–38 wt%, see Supporting Information Table S1) contained within this material and the abundance of chlorinatable nitrogen groups present in the arginine side chain (protamine is composed of 65.5% Arg residues). This ability to produce nitrogen-rich composite materials represents one of the advantages of utilizing biomimetic synthesis routes to generate materials for halamine functionalization. Indeed, protamine/silica materials may alternately be prepared by chlorinating protamine adsorbed on the surface of pre-synthesized silica microspheres. However, such materials have a substantially lower fraction of protamine (0.5–6 wt%, see Supporting Information Table S1) as compared to pSiO<sub>2</sub>-Cl and thus, possess a proportionally lower Cl content following chlorination ( $0.095 \pm 0.008$  mmol Cl/g).

Encouraged by the positive results of the pSiO<sub>2</sub> system, additional biomimetically synthesized organic/inorganic hybrids were investigated for their suitability for in situ halamine functionalization. Based on their nitrogen-rich chemistry and previous descriptions in the bioenabled materials synthesis literature, protamine/titania (pTiO<sub>2</sub>), polyethylene imine/silica

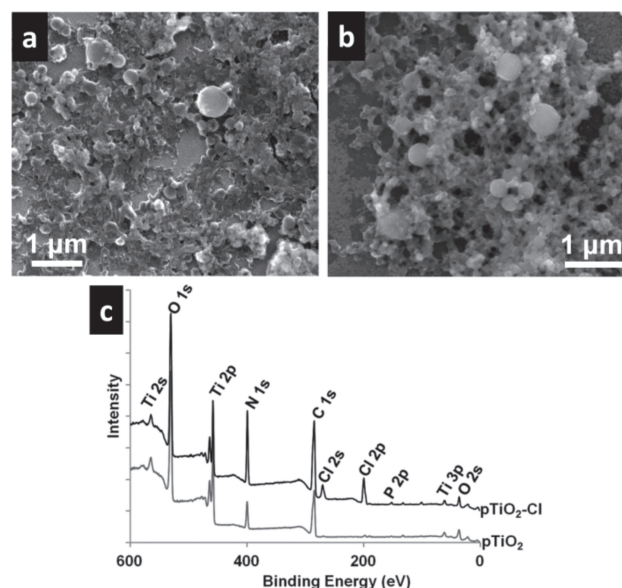


**Figure 2.** Characterization of protamine/TiO<sub>2</sub> materials before and after chlorination. SEM of a) pTiO<sub>2</sub> and b) pTiO<sub>2</sub>-Cl. c) Chemical analyses by XPS of pTiO<sub>2</sub> (bottom spectrum, gray line) and pTiO<sub>2</sub>-Cl (top spectrum, black line).

(PEISiO<sub>2</sub>), and poly-L-lysine/silica (polyKSiO<sub>2</sub>) samples were synthesized under benign, aqueous conditions.<sup>[1]</sup> The TiO<sub>2</sub> precipitates produced through the interaction of protamine with a titania precursor compound (titanium bis(ammonium lactate) dihydroxide) consisted of particles possessing diameters  $<1$   $\mu$ m that were interconnected to produce a fused network (Figure 2a and Supporting Information Figure S5). The morphology of these pTiO<sub>2</sub> materials is similar to that of the titania materials previously produced in reactions mediated by highly cationic biomolecules and utilizing the same titania precursor compound.<sup>[9,29,30]</sup> The silica precipitates produced from silicic acid under the influence of PEI and low-molecular weight poly-L-lysine were composed of aggregates of 200–2000 nm spherical and  $\approx 200$  nm irregularly shaped particles, respectively (Supporting Information Figure S6,S7). Such morphologies are comparable to those previously observed for PEISiO<sub>2</sub> and polyKSiO<sub>2</sub> materials.<sup>[31,32]</sup> The organic contents of the synthesized PEISiO<sub>2</sub> and polyKSiO<sub>2</sub> powders, as determined by CHN elemental and thermogravimetric analyses, are provided in Table S1 (Supporting Information). In each of the new systems investigated, Cl was present in samples subjected to a 1 h chlorination reaction but absent in the initial materials (Figure 2c and Supporting Information Figure S8–S10). The characterization of PEISiO<sub>2</sub>, polyKSiO<sub>2</sub>, and their chlorinated counterparts by solid state NMR spectroscopy is presented in Supporting Information Figures S11,S12. The active Cl contents of the pTiO<sub>2</sub>-Cl, PEISiO<sub>2</sub>-Cl, and polyKSiO<sub>2</sub>-Cl, as determined by iodometric titration, are presented in Table 1. As initially observed in the pSiO<sub>2</sub>/pSiO<sub>2</sub>-Cl system, the morphologies and characteristic feature sizes of the pTiO<sub>2</sub>, PEISiO<sub>2</sub>, and polyKSiO<sub>2</sub> materials were unmodified by the chlorination procedure (Figure 2 and Supporting Information Figure S5–S7). A more visually striking example of such morphology preservation was observed when



**Table 1.** The chlorine content and antimicrobial activity of several biomimetically synthesized and halamine functionalized composite materials. The powder-organism contact time was 10 min. Initial bacteria (cells or spores) cfu was  $10^8$ . Statistical analysis could not be performed for tests involving the exposure of vegetative bacterial cells to chlorinated samples as the number of viable cells was reduced to an undetectable limit. (\*) designates a single data point only, activity did not warrant extensive testing.

Material tested	mmol Cl/g material	Log reduction in cfu (compared to positive control)			
		<i>B. thuringiensis</i> spores	<i>B. thuringiensis</i> cells	<i>S. aureus</i> cells	<i>E. coli</i> cells
pSiO <sub>2</sub> -Cl	6.50 ± 0.28	6.5 ± 1.8	7	7	7
pTiO <sub>2</sub> -Cl	3.70 ± 0.25	5.0 ± 1.5	7	7	7
PEiSiO <sub>2</sub> -Cl	5.09 ± 0.18	not effective	7	7	7
polyKSiO <sub>2</sub> -Cl	3.02 ± 0.01	1.2(*)	7	7	7

hexagonal polyK/SiO<sub>2</sub> platelets (produced with high molecular weight poly-L-lysine) were chlorinated, yielding hexagonal polyKSiO<sub>2</sub>-Cl platelets (**Figure 3**).<sup>[33]</sup> X-ray diffraction characterization of pTiO<sub>2</sub>-Cl powders indicated that the conditions utilized to charge protamine with Cl had no appreciable effect on the crystalline phases present within this material (Supporting Information Figure S13).

## 2.2. Material Durability

The shelf life of N-chlorinated molecules is an important consideration in the practical application of halamine-functionalized materials. Prior studies have determined that textiles

modified with a variety of N-Cl compounds maintained stable biocidal activities when stored at room temperature for periods of time ranging from weeks to months.<sup>[21,34,35]</sup> The shelf life of chlorinated amino acids and proteins has not been previously explored however, the pot life (i.e., lifetime in aqueous solution) of these halamines has been observed to be highly dependent on protein sequence and solution temperature.<sup>[36–38]</sup> The storage stability and service lifetime of the materials produced in the current study, under adverse, real-world conditions, remains to be assessed at this time. One of the attractive features of halamine compounds is that the Cl content of these materials that may be lost during long-term storage or antimicrobial action, can be recharged.<sup>[39]</sup> Like other halamine-bearing materials, the Cl functionality of pSiO<sub>2</sub>-Cl that is consumed through chemical reactions (e.g., oxidation of biological substrates or deactivation with Na<sub>2</sub>S<sub>2</sub>O<sub>3</sub>) could be regenerated by rechlorinating the composites (see Supporting Information Table S2).<sup>[39]</sup>

## 2.3. Chlorination and Characterization of Biogenic Substrates

Given the successful chlorination of several different biomimetically synthesized materials, our interests turned to exploring the applicability of this approach to natural biominerals. As a proof-of-concept, purified cell walls of the diatom *Conscindiscus granii* were subjected to the same chlorination conditions as utilized for the biomimetically generated materials. Such purified *C. granii* cell walls (frustules) are primarily composed of silica but also contain bound, long chain polyamines (LCPAs) that display multiple sites suitable for halamine formation.<sup>[40]</sup> The intricately patterned ultrastructure of the diatom frustules was unaffected by the chlorination reaction, and Cl, which is absent in the initial frustules, was detected by XPS analysis in the chlorinated cell walls (**Figure 4**). Iodometric titration of the chlorinated frustules indicated that these materials contained  $0.01 \pm 0.001$  mmol Cl/g. Though the Cl content of the chlorinated frustules is much lower than that of pSiO<sub>2</sub>-Cl, the amount of Cl carried by these reacted biominerals is equivalent to that of chlorinated Nomex fabric, a material that has previously been used in an antimicrobial role.<sup>[24]</sup> That *C. granii* frustules can exhibit Cl loadings comparable to Nomex is impressive when considering that the latter is composed entirely of chlorinatable material, while the former is predominately unreactive SiO<sub>2</sub> (94.2 wt%, see Supporting Information Table S1).

## 2.4. Assessment of the Bactericidal and Sporocidal Activities of Chlorinated, Biomimetically Synthesized Materials

The objective of this study was to utilize the biomolecule-associated nitrogen-containing moieties within biomimetically generated hybrids to add rapid and potent antimicrobial activity to these materials. The bactericidal activity of the biomimetically synthesized and chlorinated materials generated in this study were initially assessed utilizing Gram negative *Escherichia coli* and Gram positive *Staphylococcus aureus* cells. The non-pathogenic *E. coli* and *S. aureus* strains selected for this study serve as surrogates for virulent strains, such as *E. coli* O157:H7 and methicillin-resistant *S. aureus* that are sources of infection and food- or water-borne disease.<sup>[41–43]</sup> The antimicrobial activity of the chlorinated materials is presented in Table 1. Despite the

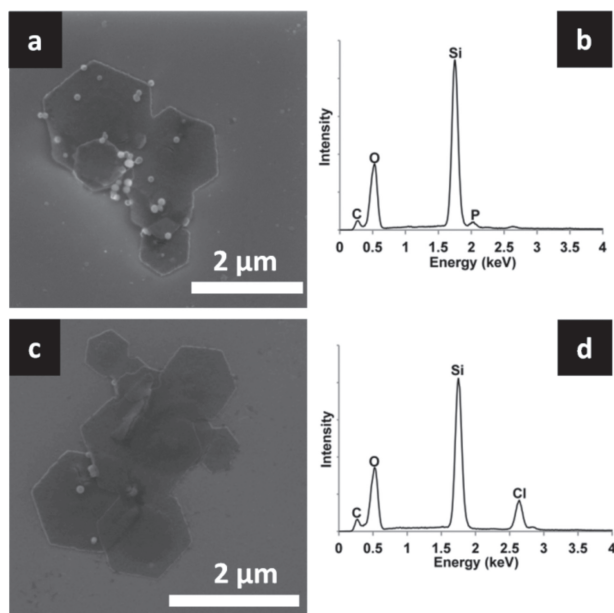


**Figure 3.** Chemical and morphological characterization of polyKSiO<sub>2</sub> hexagonal platelets before and after chlorination. a) SEM image and b) EDS analysis of polyKSiO<sub>2</sub> hexagonal platelets. c) SEM image and d) EDS analysis of chlorinated polyKSiO<sub>2</sub> hexagonal platelets. A small proportion of spherical polyKSiO<sub>2</sub> particles are also visible in a) and c).

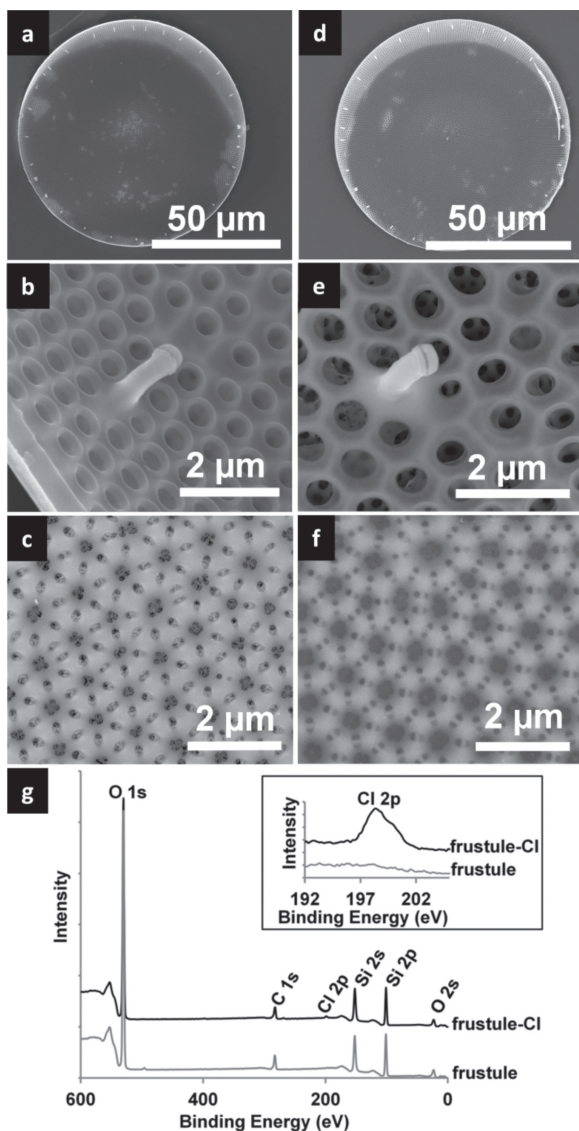


**Figure 4.** Characterization of the ultrastructure and chemistry of *C. granii* diatom frustules before and subsequent to LCPA chlorination. a–c) Representative SEM images of *C. granii* frustules. d–f) Representative SEM images of *C. granii* frustules following LCPA chlorination. The *C. granii* frustules depicted in (a–c) are not the same frustule shown in (d–f). g) XPS analyses of *C. granii* frustules before and after chlorination. High resolution XPS scan of Cl 2p region of *C. granii* frustules before and after chlorination are presented as inset in (g).

relatively small amount of biomimetically synthesized and chlorinated materials utilized (100 mg) and short contact times (10 min), each powder tested achieved a 7 Log kill (i.e., 99.99999% reduction in cfu) of *E. coli* or *S. aureus* cells (initial challenge of  $10^8$  cfu). Given this robust activity, samples of the chlorinated powders were tested against cells and spores of *Bacillus thuringiensis* Al Hakam, a Gram positive bacterium that is homologous to and used as a surrogate for *Bacillus anthracis* (the causative agent of anthrax).<sup>[44]</sup> Similar to the results observed for the activity of the chlorinated biomimetic materials against *E. coli* and *S. aureus*, all particles tested achieved a

7 Log kill of the inoculated *B. thuringiensis* cells (initial cfu of  $10^8$ ) within 10 min of contact. Bacterial spores are considerably more difficult to kill than their metabolically active counterparts, and many previously prepared halamine materials exhibit substantially reduced sporicidal activity against endospores.<sup>[17,21,22]</sup> The chlorinated protamine-based materials systems, pSiO<sub>2</sub>-Cl and pTiO<sub>2</sub>-Cl, performed exceptionally well in the rapid (10 min contact time) deactivation of these tough bacterial spores, achieving  $6.5 \pm 1.8$  and  $5.0 \pm 1.5$  Log reductions in the cfu of *B. thuringiensis* spores ( $10^8$  cfu challenge), respectively. The comparatively reduced sporicidal activity of pTiO<sub>2</sub>-Cl may be attributed to the lower level of Cl loading achieved for this material compared to pSiO<sub>2</sub>-Cl (Table 1). Nonetheless, the sporicidal activity of pTiO<sub>2</sub> is quite high, and pTiO<sub>2</sub>-Cl materials fully decontaminated (7 Log kill) challenges of *B. thuringiensis* spores ( $10^8$  cfu) when contact times were extended to 30 min. In addition to the protamine-based systems, PEISiO<sub>2</sub>-Cl and polyKSiO<sub>2</sub>-Cl were tested for, but were not found to exhibit, significant sporicidal activity. Neither unchlorinated biomimetic materials (i.e., pSiO<sub>2</sub>, pTiO<sub>2</sub>, polyKSiO<sub>2</sub>, and PEISiO<sub>2</sub>) nor their purely inorganic counterparts (i.e., SiO<sub>2</sub> and TiO<sub>2</sub>) exhibited bactericidal or sporicidal activity under the conditions of this study.

## 2.5. Mechanism of Biocidal Action

Hypochlorous acid (HOCl) and its salts (e.g., sodium hypochlorite (NaOCl)) are potent oxidizing agents that are produced on an industrial scale and used extensively to disinfect drinking water, swimming pool water, and contaminated surfaces.<sup>[45–47]</sup> Hypochlorous acid is also generated enzymatically by activated neutrophils, monocytes, and macrophages within the human body, where it serves as an antibacterial agent.<sup>[45]</sup> Though much remains to be elucidated regarding the microbicidal action of HOCl, a number of mechanisms by which hypochlorous acid kills vegetative bacteria have been established. Such mechanisms include the deactivation of bacterial enzymes by fragmenting, denaturing, and/or aggregating these proteins.<sup>[37]</sup> The catalytic activity of bacterial enzymes may additionally be extinguished by HOCl through the modification of amino acid side chain chemistries (possibly including those within the active site of the enzyme).<sup>[37]</sup> Hypochlorous acid may also kill bacteria by unfolding and aggregating thermolabile proteins, increasing the permeability of the cell membrane, disrupting ATP synthesis, and damaging DNA.<sup>[48–51]</sup> *Bacillus* spores are resistant to many chemical disinfectants however, these specialized and resilient cell types are susceptible to deactivation by hypochlorous acid and hypochlorite ions.<sup>[17,52]</sup> Mechanistically, HOCl kills *Bacillus* spores by damaging the cell's nutrient germinant receptors and cortex lytic enzymes, rendering the spores unable to germinate.<sup>[52]</sup> The germination of HOCl/OCl<sup>−</sup> treated spores may be further inhibited or blocked by the severe damage caused to the spore's inner membrane by these chemical agents.<sup>[52]</sup>

Halamine compounds, including those derived from biomolecules, retain the oxidizing capacity of HOCl and are similarly capable of damaging proteins, lipids, and DNA.<sup>[45,53]</sup> Examples of such damage include the oxidation of sulfur-containing amino acid residues (e.g., the oxidation of cysteine to cysteine

acid), the chlorination of tyrosine side chains and other aromatic compounds, lipid peroxidation, and the N-chlorination of nucleic acid bases and amino acid side chains.<sup>[53,54]</sup> Though the regeneration of hypochlorous acid from halamine compounds is possible (Scheme 1), the most predominant mode of action by these compounds is the direct transfer of Cl from the intact N-Cl compound.<sup>[55]</sup>

The bactericidal efficacies of the mineralized and chlorinated peptides explored in this study are comparable to the antimicrobial activities of halamine-charged amino acids, peptides, and proteins (i.e., silk fibroin) that have been previously documented in the literature.<sup>[26,36,56,57]</sup> All of the N-Cl charged biomimetic composites investigated in the current study possessed high bactericidal activity however, only those materials containing chlorinated protamine rapidly killed *B. thuringiensis* spores (see Table 1). The differences in the sporicidal activity of these biomimetically synthesized materials are due to the underlying chemistries of the nitrogen moieties chlorinated in each peptide or polymer. Previous research has demonstrated that the biocidal activity of a halamine compound is inversely proportional to the stability of the N-Cl bond.<sup>[58]</sup> For example, cotton fabrics modified with amide- and imide-based halamine molecules were noted to more rapidly kill *E. coli* cells than cloth similarly grafted with a chlorinated amine-bearing compound.<sup>[58]</sup> In this prior example, amine N-Cl bonds are more stable and thus, less effective in killing bacteria than amide- or imide-based N-Cl bonds.<sup>[58,59]</sup> Though longer contact times are required, materials functionalized with such amide- and imide-based halamines have also proven effective in killing *Bacillus* spores.<sup>[21,22]</sup> The N-Cl bond dissociation energy of guanidino-based compounds, such as those created through the chlorination of the arginine side chain (Figure 5), lies close to that of amide based halamines.<sup>[60]</sup> Given this similarity of bond

strengths, it is conceivable that pSiO<sub>2</sub>-Cl and pTiO<sub>2</sub>-Cl, materials that are enriched in chlorinated arginine residues, would also be capable of killing *Bacillus* spores. To the best of our knowledge, the antimicrobial activity of guanidino-based halamines has not previously been explored by the materials science community. The more rapid rate of sporicidal activity exhibited by pSiO<sub>2</sub>-Cl and pTiO<sub>2</sub>-Cl relative to materials functionalized with synthetically produced halamines may be a result of this unique guanidino N-Cl chemistry or the high density of Cl present in these materials. The identification of a definitive mechanism explaining the extremely rapid sporicidal activity of the chlorinated protamine-containing materials produced in this work requires further study and is currently under investigation.

The primary nitrogen-containing functional groups available for chlorination in the remaining biomimetically synthesized materials investigated here, PEISiO<sub>2</sub> and polyKSiO<sub>2</sub>, are amines (Figure 5). Previous research conducted with the amine-based halamine, chloramine-T, established that this compound was able to kill vegetative *Bacillus* cells but was ineffective against *Bacillus* spores due to the protective properties of the spore coat.<sup>[52,61]</sup> Mono-chloro-glycine, a compound synthesized via the chlorination of the  $\alpha$ -nitrogen of the amino acid glycine was similarly ineffective in killing *Bacillus* spores.<sup>[62]</sup> Given these prior findings, the poor spore killing capability of PEISiO<sub>2</sub>-Cl and polyKSiO<sub>2</sub>-Cl relative to pSiO<sub>2</sub>-Cl or pTiO<sub>2</sub>-Cl was not unexpected. The minor amount of sporicidal activity exhibited by polyKSiO<sub>2</sub>-Cl may stem from the chlorination of the amide groups found in the peptide backbone or the di-chlorination of  $\epsilon$ -amine group. Halamine compounds based on N-Cl amide or N-Cl<sub>2</sub> amine chemistries have been reported to exhibit sporicidal activity, though the contact times required to eliminate bacterial spores exceeds those explored in the current study.<sup>[21,22,62]</sup>

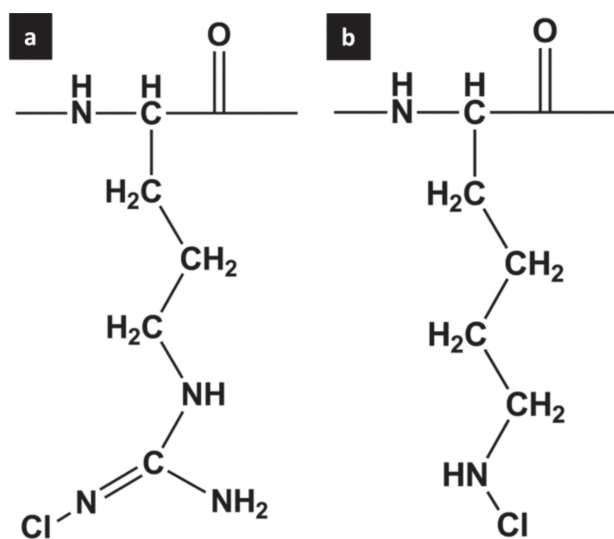


**Figure 5.** Predicted chemical structures of chlorinated amino acid residues. a) The structure of a halamine compound formed through the N-chlorination of the imine group present in the side chain of an arginine residue. b) The structure of a halamine compound formed via the mono N-chlorination of the side chain amine group present in the amino acid residue lysine.

## 2.6. Assessment of the Bactericidal Activity of Chlorinated Diatom Frustules

In addition to these biomimetically synthesized hybrids, chlorinated diatom frustules were tested for antimicrobial efficacy. As the chlorinated *C. granii* cell walls contained Cl in amounts similar to that achieved for Nomex fabric, these chlorinated biominerals were tested for bactericidal activity against *E. coli* cells at concentrations reflecting those previously used for Nomex-Cl.<sup>[24]</sup> Mirroring the antimicrobial activity of the biomimetic-Cl materials and Nomex-Cl, relatively small amounts of chlorinated diatom frustules (40 mg) achieved a 5 Log kill (i.e., 99.999% reduction in cfu) of 10<sup>6</sup> cfu of *E. coli* within 10 min of contact. Unchlorinated diatom cell walls did not display bactericidal activity. Like the PEI and poly-lysine materials described above, chlorinated *C. granii* frustules are not expected to exhibit rapid sporicidal activity, as they possess only amine-based halamines. Though effective in killing bacteria, the scope of the diatom frustules' antimicrobial activity may be further enhanced through genetic manipulation (i.e., increasing the amount of N-bearing proteins entrapped within the frustule) or via the layer-by-layer coating and mineralization of these biogenic structures with supplementary cationic biomolecules, such as protamine.<sup>[27,63]</sup> Collectively, the data presented in this study clearly demonstrates that all chlorinated biomimetic and



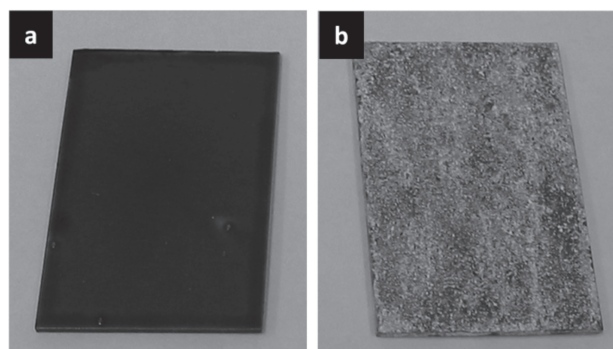


**Figure 6.** Antimicrobial paint from pSiO<sub>2</sub>-Cl. An optical photograph of borosilicate glass microscope slides coated with a) base paint (dark grey in image) and b) paint (dark grey in image) and pSiO<sub>2</sub> powder (light grey over paint). The samples shown are 37.5 mm × 25 mm in size.

biogenic composites are extremely effective in killing the tested bacterial cells, and those containing chlorinated protamine also exhibit potent sporicidal activity.

## 2.7. Application of pSiO<sub>2</sub> to Coating Technologies

To investigate the feasibility of utilizing chlorinated biomimetic materials on practical substrates for real-world applications, we explored the incorporation of pSiO<sub>2</sub>-Cl into paint to produce bactericidal coatings. The development of antimicrobial paints is aimed at reducing the spread of pathogenic organisms and nosocomial infection in clinical facilities.<sup>[23,64,65]</sup> Indeed, previous studies have demonstrated that health care workers' gloves and hands may be contaminated with multidrug-resistant pathogens as a result of touching contaminated surfaces in patient rooms.<sup>[66,67]</sup> In this study, pSiO<sub>2</sub> powders were applied to the surfaces of substrates coated with a wet commercial paint. After the paint was cured (**Figure 6**), the substrates were subsequently subjected to chlorination conditions. This procedure yielded paint-Cl or paint/pSiO<sub>2</sub>-Cl substrates that had Cl contents of  $0.0026 \pm 0.0003$  and  $0.0777 \pm 0.0285$  mmol Cl/mm<sup>2</sup>, respectively. Consistent with the activity of free pSiO<sub>2</sub>-Cl powder, paint/pSiO<sub>2</sub>-Cl coated substrates challenged with *E. coli* cells ( $10^8$  cfu) were found to reduce the number of bacterial cells to an undetectable level (7 Log kill) within 10 min of contact (Supporting Information Table S2). Conversely, painted substrates (i.e., no pSiO<sub>2</sub>) subjected to chlorination conditions did not exhibit significant antibacterial activity (Supporting Information Table S2). This result indicates that biomimetically synthesized and halamine-containing materials may be added to the surfaces of commercial paints, without adjusting paint chemistry, to add bactericidal activity to coated substrates.

One important consideration for real-world deployment is the possible toxicity of pSiO<sub>2</sub>-Cl or any of its degradation products to non-pathogenic organisms. Though pSiO<sub>2</sub>-Cl remains to be tested in this area, the results from prior studies examining the toxicity and mutagenicity of N-Cl compounds are encouraging. For example, Sun and co-workers have demonstrated that rat skin cell lines maintain excellent viability when incubated with halamine-charged nanofibers.<sup>[68]</sup> Chlorinated biomolecules

similar to those explored in the current study (i.e., peptides) have been found to be non-mutagenic (i.e., tested with *Salmonella typhimurium* strain TA100) and possess lower toxicity than other N-Cl compounds (i.e., tested with *Vibrio fischeri*).<sup>[69,70]</sup> Reports of the mutagenic and toxic nature of chlorinated amino acids (i.e., species that may be created through the degradation of N-Cl peptides) vary considerably depending on the identity of the amino acid and from study to study.<sup>[36,71–73]</sup> The leaching of chlorinated peptides from pSiO<sub>2</sub>-Cl or the other materials developed in the current study should be minimal, as these biomolecules are entrapped within an inorganic matrix. The widespread use of pSiO<sub>2</sub>-Cl in paints or other practical applications will of course require extensive additional research and testing.

## 3. Conclusions

We have communicated a facile method for the addition of antimicrobial activity to biomimetically and biologically produced organic/mineral composite structures. The processing route presented is based upon the chlorination of nitrogen moieties contained within the organic constituent of the composite material to produce halamine compounds. The morphology of biomimetically produced silica and titania particles, as well as the fine features of the diatom frustules, were unaffected by the chlorination reaction. All chlorinated materials, including Cl-loaded biominerals, were effective in rapidly killing bacterial cells, and materials containing chlorinated arginine residues (i.e., pSiO<sub>2</sub>-Cl and pTiO<sub>2</sub>-Cl) displayed potent sporicidal activity. Such halamine-functionalized biomolecule/inorganic composites may be utilized for their biocidal activity in a variety of formats including dispersible powders, paint additives, or coatings.

Considering the straightforward and inexpensive nature of the chlorination procedure and the high antimicrobial efficacies demonstrated in this study, we anticipate that the methodologies presented here will be extended to provide additional activities to a variety of multi-functional protein-templated structures. For example, the chlorination of proteins or protein cages (e.g., ferritin) associated with templated iron oxide nanoparticles may yield materials that can simultaneously disinfect and remove arsenic from water supplies.<sup>[1,74–76]</sup> Several previous studies have determined that halamine-functionalized textiles can degrade toxic chemicals such as pesticides and chemical warfare agent simulants.<sup>[77–79]</sup> Based on these previously demonstrated activities, it is reasonable to expect that pSiO<sub>2</sub>-Cl and similar materials may also be effective in mitigating dangerous organophosphorous compounds. Indeed, biomimetically generated materials functionalized in situ to bear halamines may be able to act to protect personnel, equipment, and water supplies from both chemical and biological agents. Though not explored here, the already potent biocidal activity of chlorinated biomimetic materials may yet be further enhanced via slight modifications to the methods outlined in this article. For example, protamine may be substituted for an organic species that contains both available nitrogen groups for halamine formation and native biocidal activity (i.e., antimicrobial peptides) to yield composites that retain bactericidal function between Cl chargings.<sup>[80]</sup> Additionally, it is conceivable that the inorganic component of biomimetically synthesized materials containing

chlorinated biomolecules may also be halogenated with  $\text{Cl}_{2(g)}$  to produce materials with greater total halogen content and enhanced decontamination capabilities.<sup>[81]</sup>

## 4. Experimental Section

**Synthesis of Polypeptide/Inorganic Composites:** Unless otherwise noted, all chemical reagents utilized in this study were purchased from Sigma Aldrich and used without further purification. The species utilized to catalyze the biomimetic synthesis of materials in this work were as follows: protamine sulfate salt from salmon (4.4 kDa MW, Sigma #P4020), polyethylene imine (PEI) (branched, 750 kDa MW, Sigma #181978), and poly-L-lysine (1–5 kDa MW, Sigma #P0879). The 0.2  $\mu\text{m}$  filtered, 18.2 M $\Omega$  water used throughout this work was purified from singly distilled facility water with a Barnstead Nano-Pure Infinity Ultrapure water system. The biomimetic synthesis of silica-based materials was conducted through the addition of silicic acid (freshly generated through the hydrolysis of tetramethoxysilane (TMOS) with 1 mM HCl) at a final concentration of 100 mM, to a sodium phosphate-citrate buffered (100 mM, pH 7) solution containing either protamine (3 mg/mL), poly-L-lysine (3 mg/mL), or polyethylene imine (PEI) (1 wt%). The biomimetic production of titania-based materials was conducted through the addition of titanium-bis-ammonium-lactato-dihydroxide (TiBALDH) (a water stable and soluble  $\text{TiO}_2$  precursor molecule) at a final concentration of 100 mM to a sodium phosphate-citrate buffered (100 mM, pH 7) solution containing 3 mg/mL protamine. The reaction solutions were mixed by vortexing for 10 s and rotated for 10 min at 60 rpm on a rotisserie-style rotator. The precipitated silica- or titania-based composite powders were recovered by centrifugation at 5K rpm utilizing a swinging bucket rotor and washed extensively with  $\text{H}_2\text{O}$ . The materials were subsequently frozen in liquid nitrogen and lyophilized for 16 h to produce dry powders. Hexagonal silica platelets were produced with poly-L-lysine (30–70 kDa MW, sigma #P2636) as previously described.<sup>[33]</sup>

**Chlorination of Organic/Inorganic Composite Powders:** Clorox household bleach (Clorox Company, Oakland, CA) was utilized as the chlorination source throughout this study. Organic/inorganic hybrid powders were chlorinated by exposing these materials to a chlorinating solution containing 10 vol% Clorox bleach, 0.5 M NaCl (additional), and adjusted to pH 5 through the addition of glacial acetic acid (110 mM final concentration).<sup>[26]</sup> The addition of acetic acid to the chlorination solution increases reaction kinetics by lowering the solution pH and forming the powerful chlorinating agent acetyl hypochlorite.<sup>[24,82]</sup> The presence of chloride ions (i.e., from the disassociation of NaCl) has also been previously noted to increase chlorination kinetics and the chlorine loading of N-bearing fabrics.<sup>[82,83]</sup> During the chlorination procedure, the materials were agitated by rotation on a rotisserie-style rotator. After the desired reaction time (varying from 1 to 60 min) the chlorinated powders were removed from the reaction solution by centrifugation at 5K rpm utilizing a swinging bucket rotor, and extensively rinsed with  $\text{H}_2\text{O}$ . Collection by centrifugation, rinse water decanting, and additional rinsing steps were repeated until the supernatant did not contain chlorine (typically 7 rinsing cycles), as determined by testing with KI/starch indicator papers (Fisher Scientific). The chlorinated materials were subsequently frozen in liquid nitrogen and lyophilized for 16 h in order to dry the powders.

The rechlorination of  $\text{pSiO}_2$  was conducted in the following manner: after chlorination and purification, a sub-sample of the  $\text{pSiO}_2$ -Cl powder was removed for iodometric titration analysis and the remainder of the sample was deactivated by incubation in an agitated solution of PBS containing 5%  $\text{Na}_2\text{S}_2\text{O}_3$  (deactivating agent in excess). Following deactivation, the  $\text{pSiO}_2$  materials were extensively rinsed with  $\text{H}_2\text{O}$  and chlorinated as described above, a total of 5 chlorine loading cycles were preformed.

To assess the role of protamine in the chlorination of  $\text{pSiO}_2$ ,  $\text{pSiO}_2$  powders were synthesized as described above. The purified and dried  $\text{pSiO}_2$  particles were loaded into a fused quartz crucible and heat treated at 400  $^\circ\text{C}$  for 4 h in air in order to pyrolyze the organic component of the composite. The burned out  $\text{pSiO}_2$  powders were chlorinated for 1 h according to the protocol specified for  $\text{pSiO}_2$ .

**Materials Characterization:** SEM was conducted utilizing a Quanta field emission gun microscope (FEI Corporation, Hillsboro, OR) operating at an accelerating voltage of 5–15 kV. Excessive charging necessitated that some samples be sputter coated with 3 nm of gold prior to SEM characterization. XPS was conducted with a Kratos AXIS Ultra DLD spectrometer (Kratos Analytical Inc., Manchester, UK). XPS was conducted utilizing monochromatic Al K $\alpha$  x-ray irradiation (1486.6 eV) at 120 W (10.0 mA emission current, 12.0 kV accelerating voltage), incident on the sample at 54.7 degrees relative to the sample normal. The spot size was approximately 1 mm<sup>2</sup>. Energy-dispersive X-ray spectroscopy and elemental mapping was conducted utilizing an EDAX (Mahwah, NJ) equipped on a XL-30 ESEM (FEI Corporation, Hillsboro, OR). Solid-state carbon NMR spectra were collected on a Tecmag Apollo NMR spectrometer at 125 MHz for carbon using a 2 mm probe from Revolutions NMR. Cross polarization spectra<sup>[84]</sup> were acquired with a 1 ms cross polarization time using a 50 kHz spin-locking field, 10 kHz magic-angle sample spinning, and two-pulse phase-modulated decoupling.<sup>[85]</sup> The chemical shifts were referenced to the methyl peak of hexamethyl benzene at 17.35 ppm using an external standard. Typical ssNMR spectra required 12 h of signal averaging. Carbon, hydrogen, nitrogen (CHN) elemental analysis was carried out using a Thermo Flash 2000 CHN Analyzer. Quantitative Cl elemental analysis was performed by the combustion of samples in an oxygen atmosphere followed by the titration of the evolved chlorine.

The oxidative chlorine content of untreated and chlorinated hybrid powders was assessed by iodometric titration in accordance with standard methods.<sup>[86,87]</sup> Briefly,  $\approx 100$  mg of unmodified or chlorinated hybrid powders were placed into a 50 mL centrifuge tube containing 35 mL of assay solution (350 mM acetic acid, 120 mM KI) and rotated at 30 rpm for 1 h. After 1 h, the powders were removed from the assay solution by centrifugation and discarded. The assay solution was subsequently titrated with standardized 0.1N and 0.01N  $\text{Na}_2\text{S}_2\text{O}_3$  solutions utilizing a starch indicator solution to determine the titration end point.<sup>[86,87]</sup> All values reported for powder Cl content represent the mean average of at least 3 independently prepared samples while reported error or error bars represent one standard deviation.

The evaluation of the Cl content of materials in which protamine was adsorbed on the surface of pre-synthesized silica particles was conducted in the following manner:  $\approx 100$  mg of 1  $\mu\text{m}$  diameter silica particles (Angstromspheres, Fiber Optics Center, Inc.) were incubated in a phosphate-citrate buffered solution (100 mM, pH 7) solution containing protamine (3 mg/mL) for 2 h with agitation provided by rotation on a rotisserie-style rotator. Following this incubation step, unadsorbed protamine was removed from the samples by extensively rinsing the materials with water. The chlorination, purification, and characterization of these materials were conducted in accordance with the details described for the  $\text{pSiO}_2$  system. All values reported for powder Cl content represent the mean average of at least 3 independently prepared samples while reported error or error bars represent one standard deviation.

**Examination of Bactericidal/Sporocidal Properties of Chlorinated Peptide/Inorganic Materials:** The antimicrobial testing of chlorinated organic/silica or organic/titania materials was conducted utilizing powders and several types of bacteria or bacterial spores in suspension. Triplicate experiments were conducted for each of the material types, and triplicate samples were collected in each experiment. *Bacillus thuringiensis* var. Al Hakam spore suspensions were prepared by incubating a vegetative culture for three days in 50 mL Nutrient Broth + CCY salts + glutamate at 34  $^\circ\text{C}$  with rotation at 220 rpm then washing eight times by centrifuging at 6K rpm for 5 min and re-suspending the pellet in 4 mL 0.1% Tween-80.<sup>[88]</sup> Upon the final wash, the pellet was re-suspended in 2 mL 0.1% Tween-80, divided into 4 aliquots, and frozen at  $-80$   $^\circ\text{C}$  for a minimum of one week before experimental use.<sup>[88]</sup> On each day of experimentation, the *B. thuringiensis* spores were diluted to  $10^8$  cfu/mL in sterile PBS (137 mM NaCl, 2.7mM KCl, 10 mM  $\text{Na}_2\text{HPO}_4$ , and 1.8 mM  $\text{KH}_2\text{PO}_4$ , pH 7.4). For vegetative *B. thuringiensis* var. Al Hakam cells, 24 h cultures were grown at 37  $^\circ\text{C}$  with rotation at 220 rpm in Nutrient Broth (BD Diagnostics). The bacterial cells were washed twice by centrifuging at 10K rpm for 5 min and re-suspending in



sterile PBS before diluting or concentrating to approximately  $10^8$  cfu/mL. Overnight culture enumerations were estimated using a hemacytometer to determine the appropriate dilution factor for vegetative cell cultures. One mL of each culture was then pipetted into a 2 mL micro centrifuge tube containing 100 mg of chlorinated or control powders. The powders were suspended in the solution by vortexing for 10 s followed by rotation on a rotisserie-style rotator. At 10 min, 0.5 mL of PBS + 0.3%  $\text{Na}_2\text{S}_2\text{O}_3$  was added to the test solution to neutralize any residual chlorine. After serial dilutions in a solution of 50 vol% Nutrient Broth and 50 vol% PBS containing 0.3%  $\text{Na}_2\text{S}_2\text{O}_3$ , 100  $\mu\text{L}$  of the samples from *B. thuringiensis* var. Al Hakam (spores and vegetative cells) were plated onto Nutrient Agar (Nutrient Broth with 1.5% Granulated Agar, BD Diagnostics), and incubated overnight at 37 °C. Positive control cultures and negative controls (unchlorinated biomimetically produced powders and inorganic equivalents) were tested by placing 1 mL of each culture or sterile PBS, respectively, in a 2 mL micro centrifuge tube and processing in the same manner as experimental samples.

The antimicrobial efficacy of chlorinated and control powders were also tested against *Escherichia coli* (K12) and *Staphylococcus aureus* (ATCC 25923) cells. Overnight cultures of the test organisms *E. coli* and *S. aureus* were grown in Luria-Bertani (LB) Broth, Miller (Amresco, Inc.) with shaking at 37 °C. The bacterial cells were collected by centrifugation at 5K rpm and washed twice with sterile PBS before being resuspended in a volume of PBS equal to the original culture volume, yielding solutions containing approximately  $10^8$ – $10^{11}$  cfu/mL (depending on bacterial strain). One mL of each culture was then pipetted into a 2 mL micro centrifuge tube containing 25 mg of chlorinated diatom frustules or 100 mg of biomimetically synthesized materials. The powders were suspended in the solution by vortexing for 10 s followed by rotation on a rotisserie-style rotator. At 10 min, 0.75 mL of PBS + 3%  $\text{Na}_2\text{S}_2\text{O}_3$  was added to the test solution to neutralize any residual chlorine. Serial dilutions were performed in 96-well plates containing 50 vol% LB media and 50 vol% PBS containing 3%  $\text{Na}_2\text{S}_2\text{O}_3$ . Samples were plated according to the drop plate method onto LB agar.<sup>[89]</sup> Positive control cultures were tested by placing 1 mL of each culture into a 2 mL micro centrifuge tube containing no powder samples, then processed identically to the experimental samples. Plates were incubated for 16 h at 37 °C and colonies were counted. All values reported for antimicrobial efficacy represent the mean average of at least 3 independently prepared samples while reported error or error bars represent one standard deviation.

**Diatom Culturing and Frustule Cleaning:** A *Coscinodiscus granii* diatom strain was a gift from Prof. Nils Kröger (Georgia Institute of Technology, Atlanta, Georgia, USA). The *C. granii* cultures were grown in L1 medium at 18 °C, under continuous illumination at 11 000–15 000 lux from cool white fluorescent bulbs for one week. The cultured *C. granii* diatom cells were harvested with the aid of a centrifuge (Sorvall Evolution RC, Kendro Lab Products, Asheville, NC, USA) operating at 7919 xg for 15 min. The resulting pellets containing a small amount of growth medium were then transferred to Falcon tubes (50 mL) and further centrifuged for 3 min at 1125 xg (5804R centrifuge, Eppendorf North America, Hauppauge, NY, USA). The pellets were suspended in 100 mM EDTA sodium dihydrate (BDH, Cat. No. BDH4142-500G) and then an appropriate amount of sodium dodecyl sulfate (SDS, Amresco, Solon, Ohio, USA) powder was added and dissolved to make a final SDS concentration of 1% (w/v). The resulting mixture was microwaved until the water boiled. The mixture was then taken out from the microwave and magnetically stirred for 40 min. The pellets were then extensively washed with de-ionized water. After extracting with acetone, the diatom frustules were dried under vacuum at room temperature for 3 h. The last traces of contaminating proteins were removed from the frustules by subjecting the materials to acid digestion in a 6 N HCl solution at 110 °C for 16 h. Following protein hydrolysis, the frustules were collected by centrifugation and extensively rinsed with water. The purified frustules were then frozen in liquid nitrogen and lyophilized for 16 h in order to dry the long chain polyamine (LCPA)-containing cell walls.<sup>[40]</sup>

**Antimicrobial Paints:** Borosilicate glass microscope slides (VWR International) were cut into  $\approx 25$  mm  $\times$  37.5 mm substrates. The glass substrates were cleaned by rinsing with water and isopropyl alcohol. Porcelaine 150 paint, lapis blue color (Pébéo Inc.) was coated onto the

substrates by spin coating (500 rpm for 15 s spread step, 2000 rpm for 15 s coating step). Where appropriate, the samples were immediately removed from the spin coater and dusted with  $\text{pSiO}_2$  before the paint was completely dry. The coated substrates were dried for 16 h under ambient laboratory conditions then the paint was cured according to the manufacturer's instructions at 150 °C for 35 min. Non-adherent powders were removed from the substrate surface by rinsing the samples with distilled water and blowing the surfaces off with nitrogen gas. The samples were chlorinated by placing two coated substrates in a 50 mL conical tube containing 45 mL of chlorination solution (see above) and rotated at 25 rpm for 1 h. The samples were rinsed extensively with water and dried with flowing nitrogen gas. Iodometric titration of the painted substrates was conducted as described above for  $\text{pSiO}_2$  powders. Evaluation of the antimicrobial activity of glass substrates coated with paint-Cl or paint/ $\text{pSiO}_2$ -Cl were conducted utilizing a modified AATCC (American Association of Textile Chemists and Colorists) Test Method 100–1999 described by Cao and Sun.<sup>[23]</sup> In this method, 100  $\mu\text{L}$  of *E. coli* cells ( $10^9$  cfu/mL) were deposited onto a substrate in ten 10  $\mu\text{L}$  droplets. The bacterial challenge was then “sandwiched” using another identical substrate to ensure full contact. After 10 min, the substrates were separated and placed into a 50 mL conical tube containing 25 mL of PBS containing 3%  $\text{Na}_2\text{S}_2\text{O}_3$  and vortexed for 30 s to quench the active Cl and detach adherent *E. coli* from the samples. The bacterial cells were plated and the bactericidal activity of the paint coupons determined as described above.

## Supporting Information

Supporting Information is available from the Wiley Online Library or from the author.

## Acknowledgements

This research was supported by the Air Force Office of Scientific Research (R.R.N.) and AFOSR FA9550-09-1-0669 and FA9550-10-1-0555 (YF and KHS). Partial funding for this project was also provided by DTRA (R.R.N.). The authors thank John M. Workman of the University of Dayton Research Institute for his assistance in conducting CHN and Cl elemental analysis. Distribution A: This material cleared for public release, distribution is unlimited (88ABW-2012-4581).

Received: September 30, 2012

Revised: January 9, 2013

Published online: April 5, 2013

- [1] M. B. Dickerson, K. H. Sandhage, R. R. Naik, *Chem. Rev.* **2008**, *108*, 4935–4978.
- [2] F. C. Meldrum, H. Cölfen, *Chem. Rev.* **2008**, *108*, 4332–4432.
- [3] M. Hildebrand, *Chem. Rev.* **2008**, *108*, 4855–4874.
- [4] N. Kröger, N. Poulsen, *Annu. Rev. Genet.* **2008**, *42*, 83–107.
- [5] R. L. Brutchey, D. E. Morse, *Chem. Rev.* **2008**, *108*, 4915–4934.
- [6] X. H. Wang, H. C. Schroder, W. E. G. Müller, *Int. Rev. Cell. Mol. Biol.* **2009**, *273*, 69–115.
- [7] N. Kröger, R. Deutzmann, M. Sumper, *Science* **1999**, *286*, 1129–1132.
- [8] K. Shimizu, J. Cha, G. D. Stucky, D. E. Morse, *Proc. Natl. Acad. Sci. USA* **1998**, *95*, 6234–6238.
- [9] N. Kröger, M. B. Dickerson, G. Ahmad, Y. Cai, M. S. Haluska, K. H. Sandhage, N. Poulsen, V. C. Sheppard, *Angew. Chem. Int. Ed.* **2006**, *45*, 7239–7243.
- [10] J. L. Sumerel, W. Yang, D. Kisailus, J. C. Weaver, J. H. Choi, D. E. Morse, *Chem. Mater.* **2003**, *15*, 4804–4809.
- [11] L. Betancor, H. R. Luckarift, *Trends Biotechnol.* **2008**, *26*, 566–572.
- [12] H. R. Luckarift, M. B. Dickerson, K. H. Sandhage, J. C. Spain, *Small* **2006**, *2*, 640–643.

- [13] D. M. Eby, K. E. Farrington, G. R. Johnson, *Biomacromolecules* **2008**, 9, 2487–94.
- [14] D. M. Eby, H. R. Luckarift, G. R. Johnson, *ACS Appl. Mater. Interfaces* **2009**, 1, 1553–1560.
- [15] D. M. Eby, N. M. Schaeublin, K. E. Farrington, S. M. Hussain, G. R. Johnson, *ACS Nano* **2009**, 3, 984–994.
- [16] M. B. Dickerson, C. L. Knight, M. K. Gupta, H. R. Luckarift, L. F. Drummy, M. L. Jespersen, G. R. Johnson, R. R. Naik, *Mater. Sci. Eng., C* **2011**, 31, 1748–1758.
- [17] P. Setlow, *J. Appl. Microbiol.* **2006**, 101, 514–525.
- [18] A. O. Henriques, C. P. Moran, *Ann. Rev. Microbiol.* **2007**, 61, 555–588.
- [19] K. Roberts, C. F. Smith, A. M. Snelling, K. G. Kerr, K. R. Banfield, P. A. Sleight, C. B. Beggs, *BMC Infect. Dis.* **2008**, 8, 1471–2334.
- [20] S. D. Worley, G. Sun, *Trends Polym. Sci.* **1996**, 4, 364–370.
- [21] J. Luo, Y. Y. Sun, *Ind. Eng. Chem. Res.* **2008**, 47, 5291–5297.
- [22] Z. B. Chen, J. Luo, Y. Y. Sun, *Biomaterials* **2007**, 28, 1597–1609.
- [23] Z. Cao, Y. Sun, *ACS Appl. Mater. Interfaces* **2009**, 1, 494–504.
- [24] Y. Y. Sun, G. Sun, *Ind. Eng. Chem. Res.* **2004**, 43, 5015–5020.
- [25] X. H. Ren, H. B. Kocer, S. D. Worley, R. M. Broughton, T. S. Huang, *Carbohydr. Polym.* **2009**, 78, 220–226.
- [26] M. B. Dickerson, W. Lyon, W. E. Gruner, P. A. Mirau, J. M. Slocik, R. R. Naik, *ACS Appl. Mater. Interfaces* **2012**, 4, 1724–1732.
- [27] Y. Fang, Q. Wu, M. B. Dickerson, Y. Cai, S. Shian, J. D. Berrigan, N. Poulsen, K. H. Sandhage, *Chem. Mater.* **2009**, 21, 5704–5710.
- [28] Y. Zhang, H. Wu, J. Li, L. Li, Y. Jiang, Y. Jiang, Z. Jiang, *Chem. Mater.* **2008**, 20, 1041–1048.
- [29] M. B. Dickerson, S. E. Jones, Y. Cai, G. Ahmad, R. R. Naik, N. Kröger, K. H. Sandhage, *Chem. Mater.* **2008**, 20, 1578–1584.
- [30] K. E. Cole, A. M. Valentine, *Biomacromolecules* **2007**, 8, 1641–1647.
- [31] C. Berne, L. Betancor, H. R. Luckarift, J. C. Spain, *Biomacromolecules* **2006**, 7, 2631–2636.
- [32] F. Rodriguez, D. D. Glawe, R. R. Naik, K. P. Hallinan, M. O. Stone, *Biomacromolecules* **2004**, 5, 261–265.
- [33] M. M. Tomczak, D. D. Glawe, L. F. Drummy, C. G. Lawrence, M. O. Stone, C. C. Perry, D. J. Pochan, T. J. Deming, R. R. Naik, *J. Am. Chem. Soc.* **2005**, 127, 12577–12582.
- [34] J. Luo, Y. Y. Sun, *J. Polym. Sci. Part A-Polym. Chem.* **2006**, 44, 3588–3600.
- [35] J. Lin, C. Winkelmann, S. D. Worley, J. H. Kim, C. I. Wei, U. C. Cho, R. M. Broughton, J. I. Santiago, J. F. Williams, *J. Appl. Polym. Sci.* **2002**, 85, 177–182.
- [36] W. Gottardi, M. Nagl, *J. Antimicrob. Chemother.* **2010**, 65, 399–409.
- [37] C. L. Hawkins, M. J. Davies, *Biochem. J.* **1999**, 340, 539–548.
- [38] C. L. Hawkins, M. J. Davies, *Biochem. J.* **1998**, 332, 617–625.
- [39] Z. B. Chen, Y. Y. Sun, *J. Polym. Sci. Part A-Polym. Chem.* **2005**, 43, 4089–4098.
- [40] M. Sumper, *Science* **2002**, 295, 2430–2433.
- [41] H. Leclerc, L. Schwartzbrod, E. Dei-Cas, *Crit. Rev. Microbiol.* **2002**, 28, 371–409.
- [42] B. A. Rogers, H. E. Sidjabat, D. L. Paterson, *J. Antimicrob. Chemother.* **2011**, 66, 1–14.
- [43] E. A. Eady, J. H. Cove, *Curr. Opin. Infect. Dis.* **2003**, 16, 103–124.
- [44] E. Helgason, O. A. Okstad, D. A. Caugant, H. A. Johansen, A. Fouet, M. Mock, I. Hegna, A.-B. Kolsto, *Appl. Environ. Microbiol.* **2000**, 66, 2627–2630.
- [45] D. I. Pattison, M. J. Davies, *Curr. Med. Chem.* **2006**, 13, 3271–3290.
- [46] S. J. Judd, G. Bullock, *Chemosphere* **2003**, 51, 869–879.
- [47] W. A. Rutala, D. J. Weber, *Guideline for Disinfection and Sterilization in Healthcare Facilities*, 2008 Centers for Disease Control and Prevention, Atlanta, GA **2008**.
- [48] J. Winter, M. Ilbert, P. C. F. Graf, D. Özcelik, U. Jakob, *Cell* **2008**, 135, 691–701.
- [49] S. Dukan, D. Touati, *J. Bacteriol.* **1996**, 178, 6145–6150.
- [50] W. C. Barrette, D. M. Hannum, W. D. Wheeler, J. K. Hurst, *Biochemistry* **1989**, 28, 9172–9178.
- [51] H. J. Sips, M. N. Hamers, *Infect. Immun.* **1981**, 31, 11–16.
- [52] S. B. Young, P. Setlow, *J. Appl. Microbiol.* **2003**, 95, 54–67.
- [53] C. L. Hawkins, D. I. Pattison, M. J. Davies, *Amino Acids* **2003**, 25, 259–274.
- [54] E. L. Thomas, M. B. Grisham, M. M. Jefferson, *Meth. Enzymol.* **1986**, 132, 569–585.
- [55] D. E. Williams, E. D. Elder, S. D. Worley, *Appl. Environ. Microbiol.* **1988**, 54, 2583–2585.
- [56] E. L. Thomas, *Infect. Immun.* **1979**, 25, 110–116.
- [57] E. L. Thomas, *Infect. Immun.* **1979**, 23, 522–531.
- [58] L. Qian, G. Sun, *J. Appl. Polym. Sci.* **2004**, 91, 2588–2593.
- [59] A. Akdag, S. Okur, M. L. McKee, S. D. Worley, *J. Chem. Theory Comp.* **2006**, 2, 879–884.
- [60] R. J. O'Reilly, A. Karton, L. Radom, *J. Phys. Chem. A* **2011**, 115, 5496–5504.
- [61] S. F. Bloomfield, M. Arthur, *Lett. Appl. Microbiol.* **1989**, 8, 101–104.
- [62] F. W. Tiley, R. M. Chapin, *J. Bacteriol.* **1930**, 19, 295–302.
- [63] N. Poulsen, C. Berne, J. Spain, N. Kröger, *Angew. Chem. Int. Ed.* **2007**, 46, 1843–1846.
- [64] A. Kumar, P. K. Vemula, P. M. Ajayan, G. John, *Nat. Mater.* **2008**, 7, 236–241.
- [65] J. Liang, K. Barnes, A. Akdag, S. D. Worley, J. Lee, R. M. Broughton, T.-S. Huang, *Ind. Eng. Chem. Res.* **2007**, 46, 1861–1866.
- [66] F. Trillis, E. C. Eckstein, R. Budavich, M. J. Pultz, C. J. Donskey, *Infect. Control Hosp. Epidemiol.* **2008**, 29, 1074–1076.
- [67] A. Kramer, I. Schwebke, G. Kampf, *BMC Infect. Dis.* **2006**, 6, 130.
- [68] X. Sun, L. Zhang, Z. Cao, Y. Deng, L. Liu, H. Fong, Y. Sun, *ACS Appl. Mater. Interfaces* **2010**, 2, 952–956.
- [69] H. Horth, *Identification of Mutagens in Drinking Water (EC 9105 SLD) WRC*, Marlow, Buckinghamshire, UK **1989**.
- [70] R. H. Jameel, G. R. Helz, *Environ. Toxicol. Chem.* **1999**, 18, 1899–1904.
- [71] E. L. Thomas, M. B. Grisham, M. M. Jefferson, *Meth. Enzymol.* **1986**, 132, 585–593.
- [72] S. Laingam, S. M. Froschio, R. J. Bull, A. R. Humpage, *Environ. Mol. Mutagen.* **2012**, 53, 83–93.
- [73] S. A. Salama, R. M. Snapka, *In Vivo* **2012**, 26, 501–517.
- [74] M. L. Flenniken, M. Uchida, L. O. Liepold, S. Kang, M. J. Young, T. Douglas, *Curr. Top. Microbiol. Immunol.* **2009**, 327, 71–93.
- [75] D. Faivre, D. Schüler, *Chem. Rev.* **2008**, 108, 4875–4898.
- [76] I. A. Katsoyiannis, A. I. Zouboulis, *Water Res.* **2002**, 36, 5141–5155.
- [77] X. Fei, P. F. Gao, T. Shibamoto, G. Sun, *Arch. Environ. Contam. Toxicol.* **2006**, 51, 509–514.
- [78] X. Fei, G. Sun, *Ind. Eng. Chem. Res.* **2009**, 48, 5604–5609.
- [79] B. Salter, J. Owens, R. Hayn, R. McDonald, E. Shannon, *J. Mater. Sci.* **2009**, 44, 2069–2078.
- [80] R. E. W. Hancock, H. G. Sahl, *Nat. Biotechnol.* **2006**, 24, 1551–1557.
- [81] J. A. Haggstrom, P. K. Stoimenov, K. J. Klabunde, *Chem. Mater.* **2008**, 20, 3174–3183.
- [82] M. Wayman, E. W. C. W. Thomm, *Can. J. Chem.* **1969**, 47, 2561–2567.
- [83] S. Liu, G. Sun, *Ind. Eng. Chem. Res.* **2009**, 48, 613–618.
- [84] P. A. Mirau, *A Practical Guide to the NMR of Polymers*, John Wiley Sons, Hoboken **2004**.
- [85] A. E. Bennett, C. M. Rienstra, M. Auger, K. V. Lakshmi, R. G. Griffin, *J. Chem. Phys.* **1995**, 103, 6951–6958.
- [86] Y. Y. Sun, G. Sun, *J. Appl. Polym. Sci.* **2003**, 88, 1032–1039.
- [87] A. D. Eaton, L. S. Clesceri, E. W. Rice, A. E. Greenberg, M. H. Franson, *Standard Methods for the Examination of Water & Wastewater* American Public Health Association, Washington, DC **2005**.
- [88] T. L. Buhr, D. C. McPherson, B. W. Gutting, *J. Appl. Microbiol.* **2008**, 105, 1604–1613.
- [89] B. Herigstad, M. Hamilton, J. Heersink, *J. Microbiol. Meth.* **2001**, 44, 121–129.